Effects of a nonuniform vertical profile of chlorophyll concentration on remote-sensing reflectance of the ocean

Malgorzata Stramska and Dariusz Stramski

Numerical simulations of radiative transfer were used to examine the effects of a nonuniform vertical profile of the inherent optical properties of the water column associated with the vertical profile of chlorophyll concentration, Chl(z), on the spectral remote-sensing reflectance, $R_{rs}(\lambda)$, of the ocean. Using the Gaussian function that describes the Chl(z) profile, we simulated a relatively broad range of open-ocean conditions characterized by the presence of a subsurface Chl maximum at depths greater than or equal to 20 m. The simulations for a vertically nonuniform Chl(z) were compared with reference simulations for a homogeneous ocean whose Chl was identical to the surface Chl of inhomogeneous cases. The range of values for the Gaussian parameters that produce significant differences in $R_{rs}(\lambda)$ (>5%) was determined. For some vertical structures of Chl(z) considered, the magnitude of $R_{rs}(\lambda)$ and the blue-to-green band ratios of $R_{rs}(\lambda)$ differ significantly from the reference values of homogeneous ocean (>70% in extreme cases of low surface chlorophyll of 0.02 mg m^{-3} and shallow pigment maximum at 20 m). The differences are small or negligible when the nonuniform profiles are characterized by a surface Chl greater than 0.4 mg m^{-3} or a depth of Chl maximum greater than 45 m (65 m in extremely clear waters with a surface Chl of 0.02 mg m^{-3} or less). The comparison of modeling results with the current algorithm for retrieving the global distribution of chlorophyll from satellite imagery of ocean color suggests that strong effects of the subsurface chlorophyll maximum on reflectance at low surface chlorophyll concentrations can lead to a severalfold overestimation in the algorithm-derived surface chlorophyll. Examples of field data from the Sea of Japan and the north polar Atlantic Ocean are used to illustrate various nonuniform pigment profiles and their effect on the blue-to-green ratio of $R_{rs}(\lambda)$.

OCIS codes: 010.4450, 280.0280.

1. Introduction

For various applications of ocean color measurements, it is important to understand the link between the remote-sensing reflectance of the ocean and the vertical structure of the ocean's optical properties and seawater constituents. Spectral remote-sensing reflectance $R_{rs}(\lambda)$ contains information about the properties of the oceanic surface layer whose thickness depends on the ocean's inherent and apparent optical properties. Because of this dependence, the thickness of the remotely sensed layer varies also with the wavelength of light λ at which R_{rs} is measured. Gordon and McCluney[1] showed that, in a homogeneous ocean, 90% of water-leaving photons backscattered from beneath the sea surface originate from a layer extending down to the penetration depth, z_{90}, at which the downwelling irradiance falls to 36.8% of its surface value. In natural waters, depth z_{90} can vary in a wide range from ~60 m to only a few meters (or even less) that depends primarily on water clarity and on the wavelength of the light considered.[2] Oceanographic observations indicate that the optical properties and optically significant constituents of seawater often show considerable vertical variation in the upper ocean. This vertical inhomogeneity creates a challenge for an understanding of the precise meaning of the values of ocean properties that are retrieved from remote-sensing reflectance, including the phytoplankton pigment concentration.

M. Stramska is with the Hancock Institute for Marine Studies, University of Southern California, Los Angeles, California 90089-0371. D. Stramski (stramski@mpl.ucsd.edu) is with the Marine Physical Laboratory, Scripps Institution of Oceanography, University of California at San Diego, La Jolla, California 92093-0238.

Received 18 February 2004; revised manuscript received 8 October 2004; accepted 29 October 2004.

0003-6935/05/091735-13$15.00/0

This challenge was first addressed more than 20 years ago.[3–5] Based on Monte Carlo radiative transfer simulations, Gordon and Clark[5] suggested that the reflectance of an actual ocean with vertical optical inhomogeneities can be related to the reflectance of a hypothetical homogenous ocean. Such a hypothetical homogeneous ocean has a pigment (chlorophyll a) concentration, Chl, that is equal to the depth-weighted average of the actual depth-varying chlorophyll concentration over the penetration depth, $\overline{\mathrm{Chl}}_{z_{90}}$ (the original symbol of Gordon and Clark[5] is $\overline{C}_s$). The Gordon–Clark weighting function, $g(z, \lambda)$, decreases exponentially with depth z from a value of 1 at the surface to 0.135 at z_{90}. This means that the contribution of Chl just below the surface to $\overline{\mathrm{Chl}}_{z_{90}}$ is more than sevenfold higher than the contribution coming from the penetration depth. The function $g(z, \lambda)$ involves the diffuse attenuation coefficient for irradiance, which itself is a function of z and of the wavelength of light, λ. This implies that $\overline{\mathrm{Chl}}_{z_{90}}$ depends on λ.

The hypothesis of Gordon and Clark was further examined by Gordon,[6] who used Monte Carlo simulations of radiative transfer for case 1 waters[7,8] whose optical properties were described with a refined bio-optical model parameterized by the chlorophyll concentration. He found that errors in the hypothesis ranged from a few percent to more than 20% and were smaller when both the particle absorption and the scattering coefficients covaried with the vertical changes in Chl(z) than when only the particle absorption covaried with Chl(z) and the scattering coefficient was independent of depth. Also, the deviation from the hypothesis was found to be larger for stronger vertical stratification of Chl(z) but generally smaller if the ratio of reflectances at two wavelengths were considered instead of the magnitude of reflectance at a single wavelength.

The Gordon–Clark hypothesis provides a sound theoretical framework for interpreting reflectance of a vertically inhomogeneous ocean in terms of an equivalent homogeneous ocean, but it has limitations for practical applications. To our knowledge, no algorithms are available for deriving the depth-weighted average concentration $\overline{\mathrm{Chl}}_{z_{90}}$ from remote sensing. Most current algorithms are based on the regression analysis between the *in situ*–measured reflectances and surface chlorophyll concentrations determined on discrete water samples taken near the sea surface within the top 5 or 10 m of the water column (rather than a correlation between the *in situ*–measured reflectances and $\overline{\mathrm{Chl}}_{z_{90}}$). The representative examples of such empirical chlorophyll algorithms include the Ocean Chlorophyll 4 (OC4) algorithm, which is now used for global processing of data from the Sea-viewing Wide Field of view satellite Sensor[9,10] (SeaWiFS), and the chlor_MODIS algorithm used by the NASA Terra/Aqua satellite missions for processing data from the Moderate-Resolution Imaging Spectroradiometer (MODIS) sensors.[11] These algorithms use the regression formulas for calculating the surface chlorophyll concentration from the blue-to-green ratios of ocean reflectance, which are based on large data sets from *in situ* measurements. We emphasize again that the chlorophyll products obtained from these algorithms cannot be regarded as $\overline{\mathrm{Chl}}_{z_{90}}$ because the actual chlorophyll data used to develop the regression formulas represent the pigment concentrations measured on surface samples rather than the values of $\overline{\mathrm{Chl}}_{z_{90}}$ obtained from measurements of the Chl(z) profile.

Gordon and Clark[5] also recommended that ". . . when remotely sensed concentrations are compared to surface measurements the comparison should be made with $\overline{C}_s$ [$=\overline{\mathrm{Chl}}_{z_{90}}$]; therefore, this quantity must be measured in all such field experiments." In practice, this recommendation is problematic because the concentrations calculated from the present remote-sensing algorithms do not represent $\overline{\mathrm{Chl}}_{z_{90}}$. Although more than 20 years has already passed since Gordon and Clark published their study, we are unaware of any significant field studies that focused on the analysis of $\overline{\mathrm{Chl}}_{z_{90}}$, development of in-water algorithms for estimating $\overline{\mathrm{Chl}}_{z_{90}}$ from ocean reflectance, or the kind of comparison–validation studies recommended by Gordon and Clark as quoted above. An important reason for this apparent lack of interest in $\overline{\mathrm{Chl}}_{z_{90}}$ is probably the fact that this quantity ceases to have biological significance in terms of representing the actual pigment concentrations, especially when the vertical pigment distribution is nonuniform.[12] The case of $\overline{\mathrm{Chl}}_{z_{90}}$ is further complicated by the wavelength dependency and the fact that the remote-sensing algorithms for chlorophyll retrieval typically utilize the reflectance data determined at two or more than two wavebands of light. Accurate determinations of $\overline{\mathrm{Chl}}_{z_{90}}$ in the field would require the measurements of the Chl(z) profile with (sufficiently) high resolution in depth as well as optical measurements that would permit the determination of weighting function $g(z, \lambda)$. The current methods for accurate determinations of pigment are based on the analysis of water samples taken from discrete depths rather than from continuous profiling; this limits the information on the actual Chl(z) profile and subsequent calculation of $\overline{\mathrm{Chl}}_{z_{90}}$.

Unlike for $\overline{\mathrm{Chl}}_{z_{90}}$, the biological significance can be quite readily attributed to the actual chlorophyll concentration profile, the mean water-column chlorophyll concentration,[2] or the total chlorophyll content of the photic zone.[12] Accurate retrieval of nonuniform profiles of pigment concentration or optical properties from remote-sensing reflectance is a formidable problem that has been touched on by relatively few studies.[12–15] Zaneveld[13] used an analytical approach based on a radiative transfer equation to relate the inherent optical coefficients of backscattering and beam attenuation to remote-sensing reflectance of a multilayered ocean. The relationships derived in that study appear to have a limited practical value be-

cause they involve the dependence on the ocean's apparent optical properties and volume scattering function. Recently Frette *et al.*[15] described an approach to resolving a vertical structure of oceanic waters that consists of two homogeneous layers with different chlorophyll concentrations. Their approach is based on radiative transfer simulations of the coupled atmosphere–ocean system with various Chl-dependent optical properties of the two oceanic layers. In addition to the assumptions of a two-layer model and its optical properties driven by Chl alone, their approach can be inadequate for a thick upper layer with relatively low Chl or a thinner upper layer with higher Chl. Using a simplified reflectance model, Sathyendranath and Platt[12] suggested that if independent information is available on the shape of the pigment profile, for example the parameters that describe the Gaussian curve of the Chl(z) profile, the pigment profile can be retrieved in absolute terms from an ocean color algorithm. They also showed that nonuniform pigment profiles can lead to a significant error in the retrieval of water-column (photic zone) integrated chlorophyll content.

In spite of significant advances that were made in our understanding of remote sensing of inhomogeneous ocean, the reality is that the present empirical algorithms for chlorophyll retrieval from ocean color are affected to an unknown degree by the nonuniformity of Chl(z) profiles or, in a more-general sense, by the nonuniformity of inherent optical properties (IOPs) of the water column. As mentioned above, these algorithms typically relate the surface chlorophyll concentration to the blue-to-green band ratio of remote-sensing reflectances (or normalized water-leaving radiances), which depends on the vertical structure of water-column properties. Therefore the vertical structure can affect both the scatter of data points and the general trend of such relationships. In this study we examine the effects of nonuniform profiles of IOPs associated with the nonuniform Chl(z) profile on the spectral remote-sensing reflectance $R_{rs}(\lambda)$ and band ratios of R_{rs}, using a large set of radiative transfer simulations. Our objective is to simulate a relatively broad range of open-ocean conditions characterized by the presence of a subsurface Chl maximum at depths greater than or equal to 20 m. The optically complex waters, especially the coastal marine environments where various nonphytoplankton water constituents are optically important and do not necessarily covary with Chl, are beyond the scope of our considerations. In contrast to previous studies of the effects of nonuniform pigment profile, our simulations for nonuniform Chl(z) profiles are analyzed relative to reference simulations of a homogeneous ocean whose chlorophyll concentration is identical to the surface concentration of nonuniform cases. With this approach, we quantify the range of values for the parameters of a nonuniform Chl(z) profile, which significantly affect the magnitude of $R_{rs}(\lambda)$ and the spectral ratios of $R_{rs}(\lambda)$ compared with those of a homogeneous ocean with the same surface Chl.

2. Methods

To examine the sensitivity of the remote-sensing reflectance to the vertical structure of chlorophyll concentration Chl(z), we carried out numerical simulations with the Hydrolight (version 4.1) radiative transfer model.[16,17] Our calculations were carried out for the spectrum of light from 350 to 700 nm in 10-nm intervals. All the optical quantities in this study are functions of wavelength of light λ, but, for simplicity, the dependence on λ is omitted from notation unless otherwise specifically stated. All the simulations included Raman scattering by water molecules. The boundary conditions and the IOPs of the water column were modeled by use of the library of subroutines provided with the Hydrolight code. The surface boundary conditions assumed a clear sky with a Sun zenith angle of 30° and a sea-surface roughness corresponding to a wind speed of 5 m s^{-1}. The ocean was assumed to be infinitely deep and optically homogenous below 100-m depth.

The vertical distributions of IOPs within the upper ocean were determined from chlorophyll profiles. Specifically, we used the chlorophyll profiles Chl(z) to calculate the spectral absorption, $a(\lambda, z)$, and scattering, $b(\lambda, z)$, coefficients as a function of depth z from bio-optical models. An additional set of Hydrolight simulations was made with $b(\lambda)$ constant with depth and hence independent of Chl(z). In the bio-optical models, $a(\lambda, z)$ is typically described as

$$a(\lambda, z) = a_w(\lambda) + a_p(\lambda, z) + a_{\mathrm{CDOM}}(\lambda, z), \quad (1)$$

where $a_w(\lambda)$ is the spectral absorption coefficient of pure seawater,[18,19] $a_p(\lambda, z)$ is the spectral absorption coefficient of particulate matter at depth z, and $a_{\mathrm{CDOM}}(\lambda, z)$ is the spectral absorption coefficient of colored dissolved organic matter (CDOM) at z. We used a subroutine abcase1 of Hydrolight code, in which the absorption components are defined as

$$a_p(\lambda, z) = 0.06 a_c^*(\lambda)\mathrm{Chl}(z)^{0.65}, \quad (2)$$

$$a_{\mathrm{CDOM}}(\lambda, z) = 0.012\mathrm{Chl}(z)^{0.65}\exp[-0.014(\lambda - 440)], \quad (3)$$

where $a_c^*(\lambda)$ is a nondimensional chlorophyll-specific absorption coefficient of phytoplankton at λ,[20,21] Chl(z) is given in milligrams of chlorophyll a per cubic meter, and λ is in nanometers. In this description of absorption, nonphytoplankton particles appear to be included in a_{CDOM}. The spectral scattering coefficient is represented as the sum of two components:

$$b(\lambda, z) = b_w(\lambda) + b_p(\lambda, z), \quad (4)$$

where $b_w(\lambda)$ is the spectral scattering coefficient of pure seawater[22] and $b_p(\lambda, z)$ is the spectral scattering coefficient of particulate matter at z taken from Gordon and Morel[8]:

$$b_p(\lambda, z) = (550/\lambda)0.30\ \mathrm{Chl}(z)^{0.62}. \quad (5)$$

In addition to absorption and scattering coefficients, the model inputs include the scattering phase function. In all the simulations the scattering phase function was described as the sum of contributions by pure seawater and particles. The particle component was taken as the average particle phase function from measurements made by Petzold[23] as described by Mobley.[16] This single phase function was used for all depths and light wavelengths.

The vertical profiles of Chl(z) were approximated by a Gaussian function superimposed upon a constant background[24]:

$$\mathrm{Chl}(z) = \mathrm{Chl}_0 + h/[\sigma(2\pi)^{0.5}]\exp[-(z - z_{\max})^2/2\sigma^2], \quad (6)$$

where Chl_0 is the background value of Chl (in milligrams per cubic meter), $z_{\max}$ is the depth of the Chl maximum (in meters), σ is the standard deviation that controls the thickness of the Chl peak (i.e., 95% of the integrated biomass is located within a water layer of thickness equal to 4σ), and $\mathrm{Chl}_{\max} = h/[\sigma(2\pi)^{0.5}]$ determines the amplitude of the Chl maximum above the value of Chl_0. The units for σ and h are meters and milligrams per square meter, respectively. Note that the actual chlorophyll concentration at the maximum can be calculated as the sum of Chl_0 and $\mathrm{Chl}_{\max}$. Equation (6) is sufficiently versatile to describe a variety of profiles found in field data with a reasonable approximation.[25] Examples of idealized chlorophyll profiles obtained from Eq. (6), which were used in our Hydrolight simulations, are shown in Fig. 1. The corresponding example profiles of IOPs, that is, the absorption and scattering coefficients at 445 nm, are also shown.

The analysis of variations in the remote-sensing reflectance caused by the Chl(z) profiles was carried out in the following way: In the first step we simulated a series of Chl(z) profiles by using the set of parameters listed in Tables 1 and 2. For each pair of values of $z_{\max}$ and Chl_0 (Table 1), the calculations were made for five values of σ (from 2 to 6 m) and a set of five values of h for each σ (Table 2). The selected h and σ values yielded the amplitude of the chlorophyll maximum, $\mathrm{Chl}_{\max}$, at 1–5 mg m^{-3}. Overall we considered 36 pairs of $z_{\max}$ and Chl_0 values. We used ten values of $z_{\max}$, from 20 to 65 m at 5-m intervals, and six values of Chl_0 from 0.02 to 0.4 mg m^{-3}. The reasons for not considering $z_{\max} > 65$ m and $\mathrm{Chl}_0 > 0.4$ mg m^{-3} are explained below. Note also that, within the ranges of $z_{\max}$ and Chl_0 considered, we used a decreasing number of Chl_0 values with increasing $z_{\max}$, as given in Table 1. As a result, we did not make the Hydrolight simulations when the influence of vertical structure of Chl(z) on R_{rs} became negligible. For each pair of $z_{\max}$ and Chl_0 values we generated 25 Chl(z) profiles determined by various combinations of σ and h, except when $z_{\max} = 20$ m, for which we generated 20 Chl(z) profiles. When $z_{\max} = 20$ m, no calculations were made for $\sigma = 6$ m because the surface Chl would differ significantly from the background value of Chl_0.

Following the scheme described above, we generated 870 profiles of Chl(z). For each of these profiles the surface chlorophyll concentration is essentially the same as the background value Chl_0. It is important to note that the parameters of the profiles were selected to cover a relatively broad range, representative of ocean conditions characterized by the presence of a subsurface Chl maximum located at depths greater than or equal to 20 m. As shown by the results below, such depths of Chl maximum imply a need to consider only the surface Chl values that are smaller than 0.4 mg m^{-3} because, for higher surface Chl, the effects of nonuniform profiles on surface reflectance are quite small. Also, we do not report on results for $z_{\max} > 65$ m because our simulations showed that, when the chlorophyll maximum is located at such large depths, the effect of the Chl(z) profile on surface reflectance is negligible. Figure 1 shows 10 of the 25 profiles for one example set of $z_{\max}$ and Chl_0 used in our simulations.

Having determined the Chl(z) profiles, we carried out the Hydrolight simulations in the next step of our approach. First, we made six Hydrolight simulations, which can be regarded as reference simulations of homogeneous ocean. Each of these reference simulations was made for uniform distribution of Chl with depth; i.e., the IOPs were constant with depth. Six values of Chl used in the reference simulations were 0.02, 0.05, 0.1, 0.2, 0.3, and 0.4 mg m^{-3}. Importantly, these values correspond exactly to the background Chl_0 values of nonuniform Chl(z) profiles. Next, we carried out two sets of Hydrolight simulations for nonuniform vertical profiles of Chl(z). In the first set of Hydrolight simulations we assumed that both the absorption and the scattering coefficients, $a(z)$ and $b(z)$, respectively, covaried with Chl(z) according to bio-optical models built into the Hydrolight code as described above. We simulated the radiative transfer for each Chl(z) profile, so we made 870 Hydrolight simulations for the $a(z)$ and $b(z)$ profiles covarying with Chl(z). In the second set of Hydrolight simulations for nonuniform Chl(z) profiles, absorption profiles $a(z)$ were calculated from Chl(z) as above, but scattering coefficient b was assumed constant throughout the entire water column. Specifically, we calculated b from the bio-optical model, using the Chl_0 values as input, so here b was the same as in the reference Hydrolight simulations for a homogeneous ocean. In this second set of simulations we again made 870 Hydrolight runs for Chl(z) profiles summarized in Tables 1 and 2. The simulations with the depth-independent b were used to account for the fact that the vertical profiles of scattering in the upper ocean do not necessarily covary with Chl. Such observations of the noncorrelation of the vertical structure of light scattering and chlorophyll were made in the open-ocean waters,[26] where a Chl maximum at depth can be induced, to a large degree, by an in-

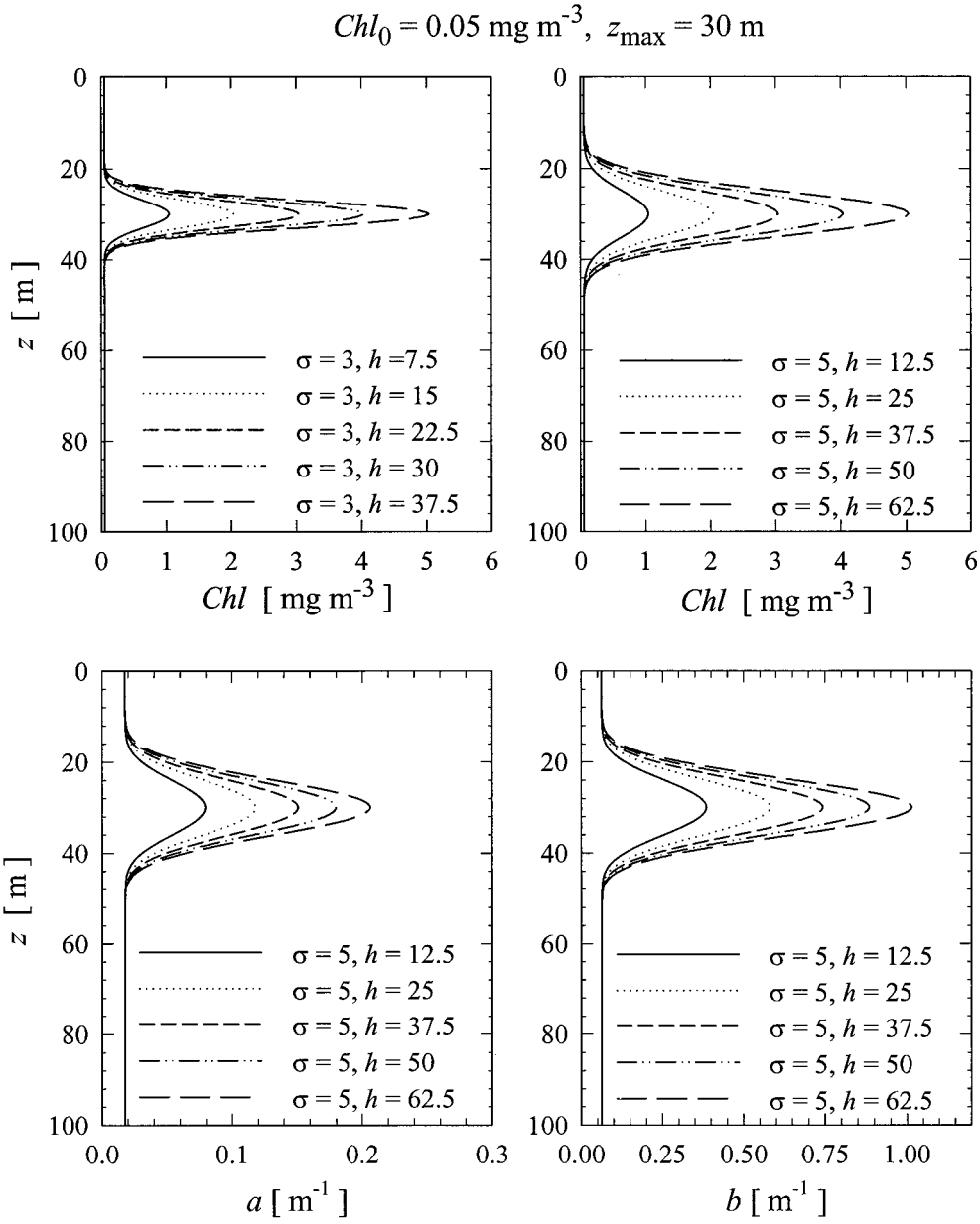

Fig. 1. Examples of chlorophyll profiles for one selected pair of z_{max} and Chl_0 values and several combinations of σ and h values as indicated. Shown also are the profiles of the absorption, a, and scattering, b, coefficients at 445 nm associated with the Chl profiles that are displayed in the top right-hand figure.

crease in chlorophyll a content in individual phytoplankton cells rather than by the concentration of cells.

Finally, we used the results from Hydrolight simulations to calculate the relative differences between nonuniform and uniform Chl profiles for the magnitude of the spectral remote-sensing reflectances, $R_{rs}(\lambda)$, and the spectral-band ratios of R_{rs}. As an example, the differences between the nonuniform Chl(z) profiles with $Chl_0 = 0.05$ mg m^{-3} and the uniform profile with Chl(z) = 0.05 mg m^{-3} were calculated. Similar calculations of the differences were made for the five remaining values of Chl_0.

Table 1. Pairs of z_{max} and Chl_0 Values Used to Generate Idealized Chl Profiles[a]

	z_{max}									
Chl_0	20	25	30	35	40	45	50	55	60	65
0.02	X	X	X	X	X	X	X	X	X	X
0.05	X	X	X	X	X	X	X			
0.1	X	X	X	X	X	X				
0.2	X	X	X	X	X	X				
0.3	X	X	X	X	X					
0.4	X	X								

[a]X indicates the pair of z_{max} and Chl_0 values for which the calculations were made.

Table 2. Pairs of σ and h Values Used to Generate Idealized Chl Profiles

	$Chl_{max} = 1$	$Chl_{max} = 2$	$Chl_{max} = 3$	$Chl_{max} = 4$	$Chl_{max} = 5$
$\sigma = 6$	$h = 15$	$h = 30$	$h = 45$	$h = 60$	$h = 75$
$\sigma = 5$	$h = 12.5$	$h = 25$	$h = 37.5$	$h = 50$	$h = 62.5$
$\sigma = 4$	$h = 10$	$h = 20$	$h = 30$	$h = 40$	$h = 50$
$\sigma = 3$	$h = 7.5$	$h = 15$	$h = 22.5$	$h = 30$	$h = 37.5$
$\sigma = 2$	$h = 5$	$h = 10$	$h = 15$	$h = 20$	$h = 25$

3. Modeling Results

First, we discuss the results from Hydrolight simulations, in which we assumed that the absorption and scattering coefficients covary with Chl(z). Figure 2 shows four examples of such results. Each example represents one pair of z_{max} and Chl_0 values and provides a comparison of the uniform Chl profile with $Chl(z) = Chl_0$ and the 20 nonuniform profiles with various combinations of σ and h. The effect of the subsurface chlorophyll maximum is to decrease R_{rs} in the blue spectral region and to increase R_{rs} in the green spectral region compared with those in the uniform Chl profile (Fig. 2, left). As a result, the $R_{rs}(\lambda)/R_{rs}(555)$ ratio in the presence of the chlorophyll maximum is reduced for wavelengths λ from the blue spectral region (Fig. 2, right). Therefore the blue-to-green ratio of reflectance can be significantly lower in the presence of the subsurface chlorophyll maximum than in the uniform profile. The effect of the chlorophyll maximum becomes more pronounced with a decrease in z_{max} and Chl_0 (see $z_{max} = 20$ m and $Chl_0 = 0.05$ mg m^{-3} in Fig. 2). If z_{max} or Chl_0 or both are sufficiently high, the differences between $R_{rs}(\lambda)$ or $R_{rs}(\lambda)/R_{rs}(555)$ observed in a vertically homogenous ocean [with $Chl(z) = Chl_0$] and a vertically inhomogeneous ocean (with background Chl_0) are small (see $z_{max} = 30$ m and $Chl_0 = 0.4$ mg m^{-3} in Fig. 2).

The influence of parameters σ and h on remote-sensing reflectance is illustrated in Fig. 3. Example results expressed as the relative change in $R_{rs}(445)$, $R_{rs}(555)$, and $R_{rs}(445)/R_{rs}(555)$ are plotted for clear surface waters, with $Chl_0 = 0.05$ mg m^{-3} and $z_{max} = 30$ m. The value of the relative change (in percent) was estimated as

$$R_{change}(\%) = [(R_{nonunif} - R_{unif})/R_{unif}]100, \qquad (7)$$

where R denotes $R_{rs}(445)$, $R_{rs}(555)$, or $R_{rs}(445)/R_{rs}(555)$, and the subscripts nonunif and unif refer to the nonuniform and uniform Chl(z) profiles, respectively. The main consequences of variation in parameters σ and h are as follows: When h increases, the biomass within the Chl peak increases relative to the background Chl_0, and as a result the magnitude of R_{change} increases as well. Increasing σ broadens the Chl maximum, which results in an increase in Chl(z) near the water surface. This also results in an increase in R_{change}. For $\sigma = 5$ m and $Chl_{max} = 5$ mg m^{-3} ($h = 62.5$ mg m^{-2}), $R_{rs}(445)$ is lower by ~17%, $R_{rs}(555)$ is higher by 16%, and $R_{rs}(445)/R_{rs}(555)$ is lower by 28% than in the uniform profile with $Chl(z) = 0.05$ mg m^{-3} (see the rightmost open circles in Fig. 3). If, however, the Chl peak is narrow ($\sigma = 2$ m) and Chl_{max} is 1 mg m^{-3} ($h = 5$ mg m^{-2}), R_{change} is less than 10% (see the leftmost open triangles in Fig. 3).

Figures 2 and 3 showed merely examples of the effects caused by different parameters of the Chl(z) profile. Based on the entire set of results from Hydrolight simulations, we can establish a domain for the parameter values of the Chl(z) profile for which the subsurface chlorophyll maximum has a significant effect on R_{rs}. A summary of such results for the case when the chlorophyll maximum produces the absolute values of $|R_{change}| > 5\%$ for $R_{rs}(445)$ is shown in Fig. 4. The choice of a 5% threshold is consistent with the current goal of accuracy in retrieving R_{rs} from satellite measurements to within $\pm 5\%$ of the true value.[27,28] Each line in Fig. 4A represents a pair of z_{max} and Chl_0 values, as indicated. Each line also connects the data points of Chl_{max} and σ, whose values can be identified from the vertical and horizontal axes of the graph, respectively. For any given line, i.e., for any given pair of z_{max} and Chl_0 values, the conditions when $|R_{change}| > 5\%$ are defined by the values of Chl_{max} and σ, which are located on the line itself as well as within the space on the right-hand side of the line. For example, line 4 represents $z_{max} = 30$ m and $Chl_0 = 0.1$ mg m^{-3}, and it connects two data points ($\sigma = 2$ m, $Chl_{max} = 2$ mg m^{-3}) and ($\sigma = 3$ m, $Chl_{max} = 1$ mg m^{-3}). In this case $|R_{change}|$ is greater than 5% for all pairs of Chl_{max} and σ on line 4 as well as for all pairs of Chl_{max} and σ located within the space to the right of line 4. The shaded area in Fig. 4B is an example illustration of the domain of Chl_{max} and σ values that produce $|R_{change}| > 5\%$. This example illustration is for $z_{max} = 20$ m and $Chl_0 = 0.4$ mg m^{-3}. We also note that $|R_{change}|$ is always greater than 5% for a given z_{max} if Chl_0 is smaller than the lowest value of Chl_0 associated with a given z_{max} in Fig. 4A. Specifically, $|R_{change}|$ is greater than 5% for $z_{max} = 20$ m and $Chl_0 < 0.4$ mg m^{-3}, for $z_{max} = 25$ m and $Chl_0 < 0.2$ mg m^{-3}, for $z_{max} = 30$ m and $Chl_0 < 0.1$ mg m^{-3}, etc. In summary, when $Chl_0 > 0.4$ mg m^{-3} and $z_{max} > 20$ m the influence of the subsurface chlorophyll maximum on R_{rs} is always small, regardless of values of σ and h. In clear waters with $Chl_0 = 0.05$ mg m^{-3}, the influence of the chlorophyll maximum on R_{rs} becomes small if z_{max} is 45 m or more. If $z_{max} = 60$ m and $Chl_0 = 0.02$ mg m^{-3}, $|R_{change}|$ is still ~5% for $R_{rs}(415)$ and $R_{rs}(445)$ but is negligible at longer wavelengths.

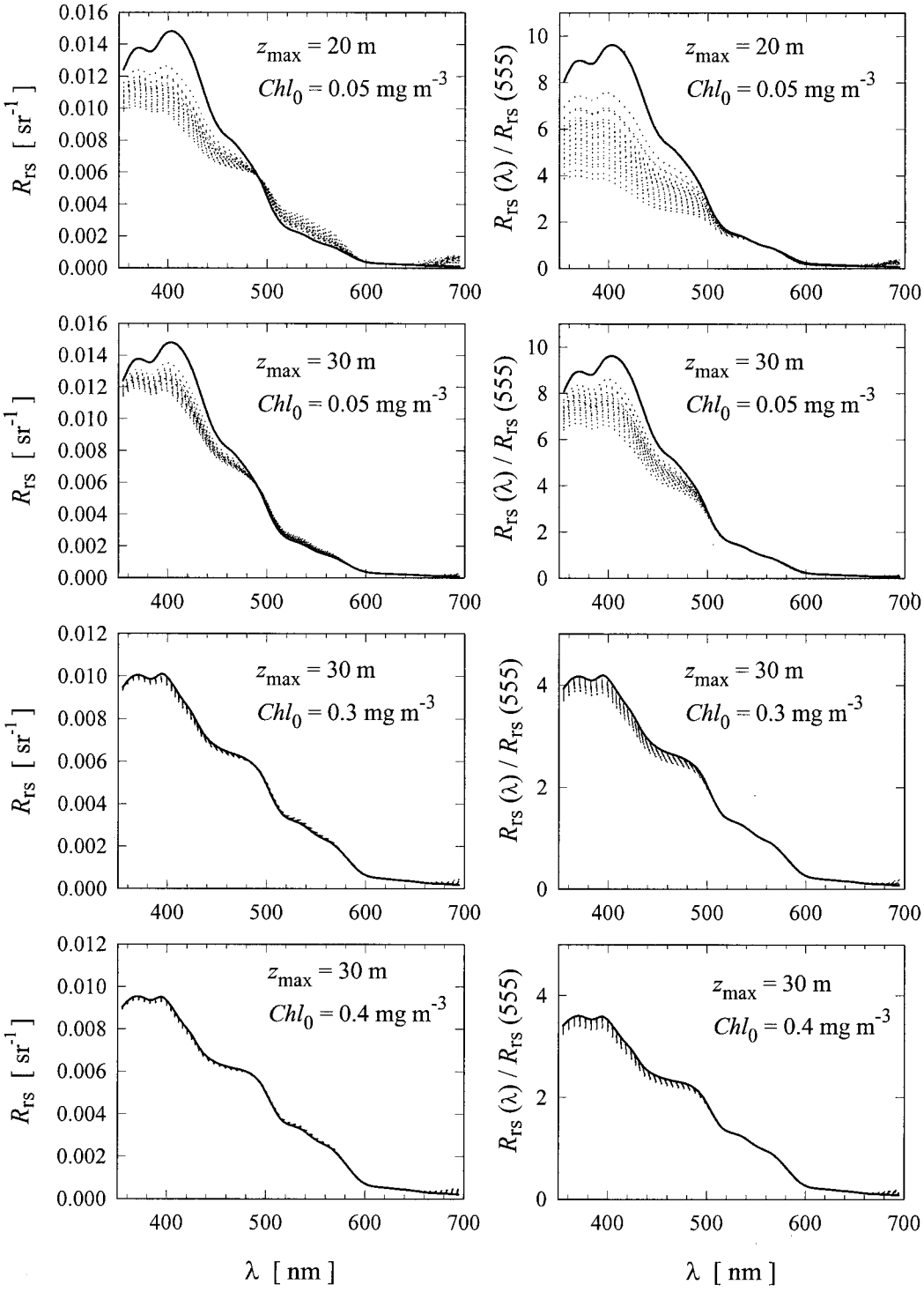

Fig. 2. Example results of radiative transfer simulations, showing the differences in reflectance $R_{rs}(\lambda)$ and reflectance ratio $R_{rs}(\lambda)/R_{rs}(555)$ between the homogenous ocean with a uniform pigment profile (solid curves) and the inhomogeneous ocean with a distinct subsurface chlorophyll maximum (dotted curves). The surface chlorophyll in the inhomogeneous case is identical to that in the homogeneous case in these simulations. The values of the chlorophyll profile parameters, z_{max} and Chl_0, are given. The simulations for nonuniform pigment profiles were made with depth-dependent absorption and scattering coefficients (see text for a detailed explanation).

Figures 5 and 6 show the domain of parameter values of the Chl(z) profile for which the subsurface chlorophyll maximum produced $|R_{change}| > 5\%$ in the ratios $R_{rs}(445)/R_{rs}(555)$ and $R_{rs}(485)/R_{rs}(555)$. We chose to present these results because these ratios are similar to those commonly used in ocean color algorithms for determining Chl. These figures can be interpreted in a way similar to that above with regard to Fig. 4 (see an example interpretation of Fig. 4B above). Figures 5 and 6 show that $|R_{change}|$ is less than 5% for

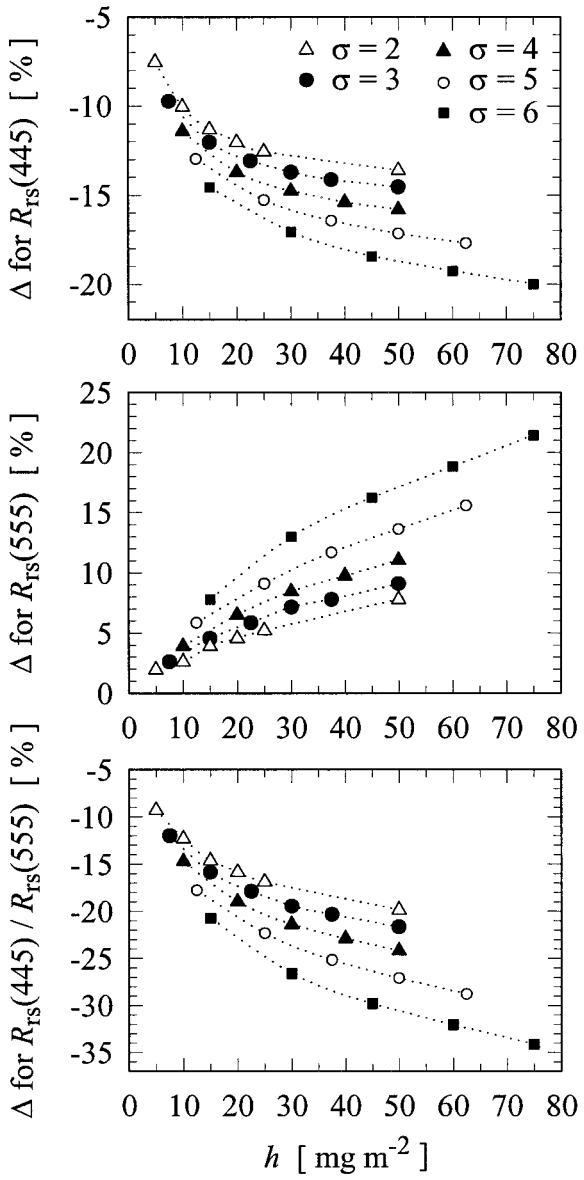

Fig. 3. Example results of radiative transfer simulations, showing how the relative difference between nonuniform and homogenous ocean values of $R_{rs}(445)$, $R_{rs}(555)$, and $R_{rs}(445)/R_{rs}(555)$ depend on parameters h and σ for a given $Chl_0 = 0.05$ mg m^{-3} and $z_{max} = 30$ m. The simulations for nonuniform pigment profiles were made with the depth-dependent absorption and scattering coefficients. The symbol Δ on the vertical axis is equivalent to R_{change} [see Eq. (7) and text for a detailed explanation].

both reflectance ratios if $Chl_0 > 0.4$ mg m^{-3} and $z_{max} > 25$ m, regardless of values of σ and h. In very clear waters with $Chl_0 = 0.02$ mg m^{-3}, $|R_{change}|$ becomes less than 5% for $z_{max} > 60$ m. In extreme cases of low surface chlorophyll of 0.02 mg m^{-3} and a shallow chlorophyll maximum at 20 m, $|R_{change}|$ can exceed 70%.

We now briefly discuss the results of the Hydrolight simulations for the situations when scattering coefficient b was constant with depth and independent of the Chl(z) profile. Recall that in these cases the absorption coefficient still covaried with Chl(z) but the depth-independent scattering coefficient was estimated simply from the surface Chl (=Chl_0). We found that in general there are larger differences in R_{rs} in the blue spectral region between the uniform and the nonuniform Chl(z) profiles for depth-independent b than for nonuniform $b(z)$ covarying with Chl(z). This result is qualitatively consistent with the conclusions of Gordon.[6] For the nonuniform Chl(z) with a constant scattering coefficient, R_{rs} decreases in both the blue and the green spectral regions compared with the uniform Chl profile. This behavior is expected because the changes in R_{rs} in our simulations are driven only by changes in the vertical profile of the absorption coefficient, as the scattering coefficient is constant with depth. It is, however, interesting to note that the differences in the reflectance band ratios between the uniform and the nonuniform Chl(z) profiles were similar, regardless of whether the scattering coefficient was constant or variable with depth. This result can be explained by the fact that, even if both the scattering and the absorption coefficients covary with Chl(z), the blue-to-green reflectance ratio is driven largely by the green-to-blue ratio of absorption coefficients. Therefore our main conclusions about R_{change} for the ratios $R_{rs}(445)/R_{rs}(555)$ and $R_{rs}(485)/R_{rs}(555)$ (Figs. 5 and 6) are expected to hold under conditions when the scattering coefficient is not correlated with Chl(z).

4. Examples of Field Data

To place our modeling results in the proper context of field observations, we now present examples of *in situ* data of Chl and reflectance ratio with an emphasis on conditions when a distinct subsurface chlorophyll maximum occurred. The data were collected in the Sea of Japan in the summer of 1999 and in the north polar waters of the Atlantic Ocean in the summers of 1998 and 1999. Methods consistent with the SeaWiFS protocols[28] were used to collect the optical data during these cruises. Among the various quantities measured, included were the underwater vertical profiles of downwelling irradiance, $E_d(z, \lambda)$, and upwelling radiance, $L_u(z, \lambda)$, which allowed the calculation of the spectral remote-sensing reflectance, $R_{rs}(\lambda)$. In the Sea of Japan the radiometric measurements were made with a MER-2048 spectroradiometer (Biospherical Instruments, Inc.), and the vertical profiles of spectral absorption, $a(z, \lambda)$, and the beam attenuation coefficient, $c(z, \lambda)$, were measured with an ac-9 meter (WetLabs, Inc.). On the cruises in the north polar Atlantic,[29] the radiometric measurements were made with the SPMR free-fall spectroradiometer (Satlantic, Inc.) and the profiles of $a(z, \lambda)$ and $c(z, \lambda)$ were measured with a-βeta sensors (HobiLabs, Inc) and c-star beam transmissometers (WetLabs, Inc.). In both regions the chlorophyll a concentration was measured in discrete water samples from selected depths by fluorometric (Sea of Japan[30]) and spectrophotometric (north polar Atlantic[29]) methods. The water samples for pigment determinations were taken shortly before or after the optical casts.

Figure 7 shows examples of nonuniform profiles of Chl(z) for two stations in the Sea of Japan and four

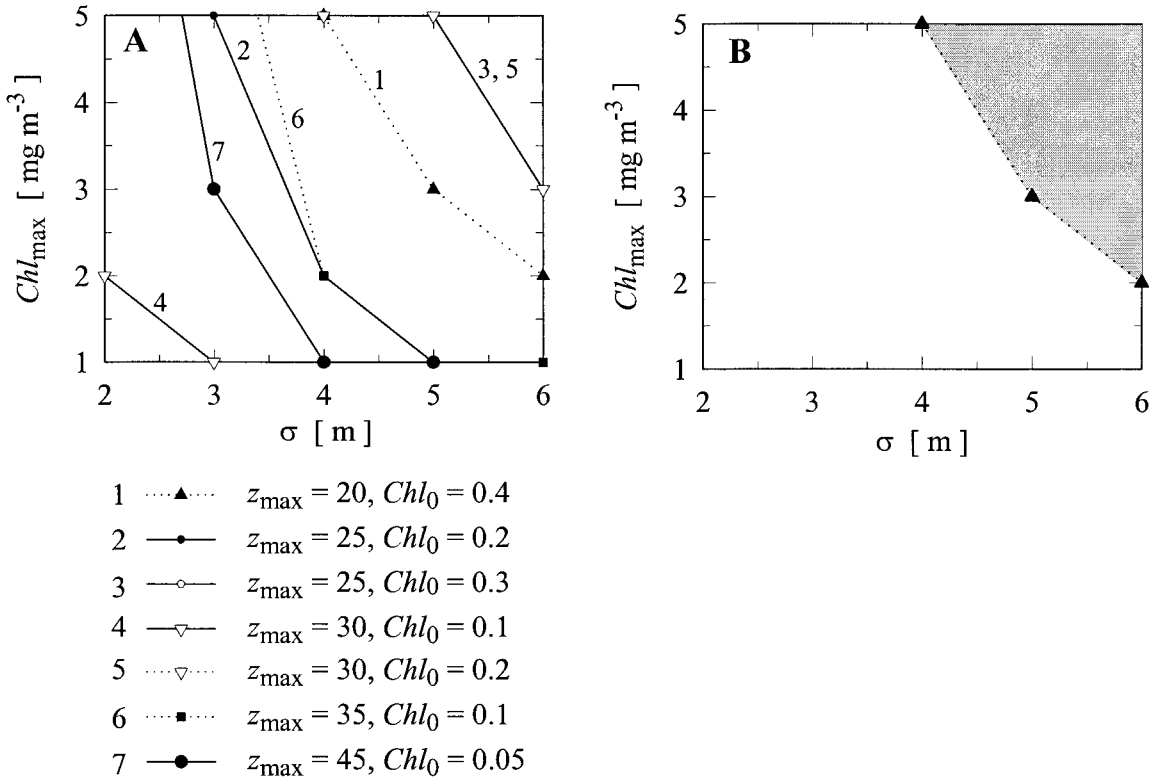

Fig. 4. A, Results of radiative transfer simulations indicating the values of σ and Chl_{max} for which the absolute value of the difference between remote-sensing reflectance $R_{rs}(445)$ in the inhomogeneous ocean and in the homogeneous ocean was greater than 5%. For a given z_{max} and Chl_0 (legend below A), all pairs of values of Chl_{max} and σ that lie on the corresponding line and to the right of the line define the domain of the Chl_{max} and σ values where the difference is >5%. B, For example, the interpretation of the figure is illustrated for line 1 from A. The shaded area corresponds to the difference >5%. The simulations for nonuniform pigment profiles were made with the depth-dependent absorption and scattering coefficients (see text for a detailed explanation).

stations in the north polar Atlantic. These Chl(z) profiles were estimated from vertical measurements of the absorption coefficient at 442 nm, or, if $a(442, z)$ was not available (as was the case for the 1998 cruise in the north Atlantic), from beam attenuation coefficient $c(442, z)$. The measurements of $a(442)$ and $c(442)$ included several data points per 1-m interval in depth, but these original data were processed to yield the final data with a 1-m resolution. Next, a regression formula (not shown here) between the measured $a(442)$ or $c(442)$ and the measured Chl was established for each station separately by use of the data from discrete depths at which Chl was determined. Then these station-specific regression equations were used to convert the $a(442, z)$ or $c(442, z)$ profiles into the Chl(z) profiles with 1-m vertical resolution. Next, we used these experimental profiles of Chl(z) to estimate the parameters of the Gaussian curve, h, σ, Chl_0 and z_{max}, by fitting Eq. (6) to the data points. Note that the examples presented in Fig. 7 cover quite a broad range of these parameters.

Based on these determinations of Gaussian parameters and the Hydrolight simulations described in Section 3, we suspect that the vertical structure of Chl(z) had a significant effect on the blue-to-green reflectance ratio in some examples shown in Fig. 7. Specifically, we suspect that the reflectance ratio could have been reduced by ~10% compared with that of the uniform profile of Chl(z) for stations 38 and 61 in the Sea of Japan and stations ks10 and ks23 in the north polar Atlantic. In contrast, the values of h, σ, Chl_0, and z_{max} for the Chl(z) profiles from stations z1 and z3 in the north Atlantic suggest that the reflectance ratio was probably unaffected by the chlorophyll maximum, even though Chl_{max} was quite high at these stations. This is so because these stations were characterized by a relatively high concentration of chlorophyll at the surface (~1 mg m^{-3}), which conceals the effect of Chl_{max} on surface reflectance.

The relationship between the measured surface Chl and the measured $R_{rs}(442)/R_{rs}(555)$ ratio in the Sea of Japan and the north polar Atlantic is illustrated in Fig. 8. Much of the seemingly random variability in the data points is caused by the fact that chlorophyll concentration in water is not the one and only variable that determines the reflectance ratio. Other factors include variability in phytoplankton composition and nonphytoplankton seawater constituents such as CDOM, organic detrital particles, and minerogenic particles. The main purpose of Fig. 8 is to demonstrate that the vertical profiles of IOPs associated with a nonuniform Chl(z) profile can also

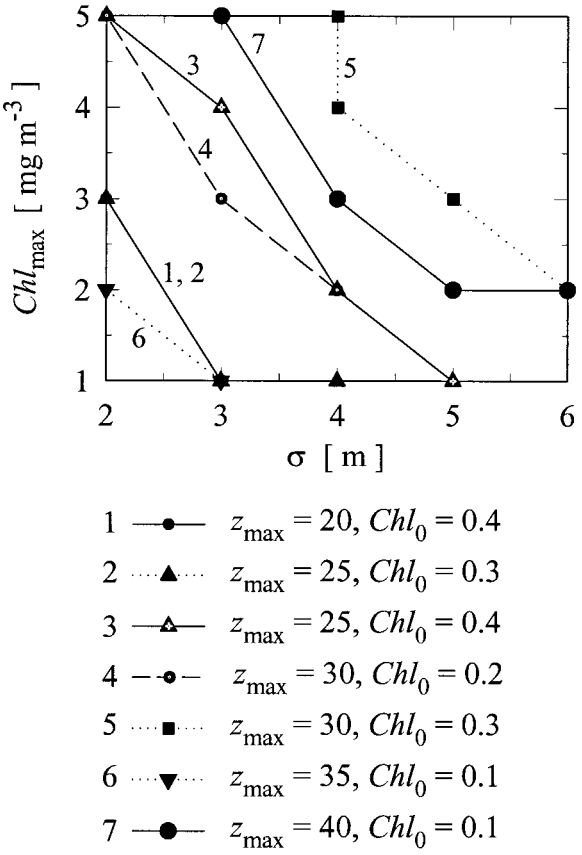

Fig. 5. Same as Fig. 4 but for the remote-sensing reflectance ratio $R_{rs}(445)/R_{rs}(555)$.

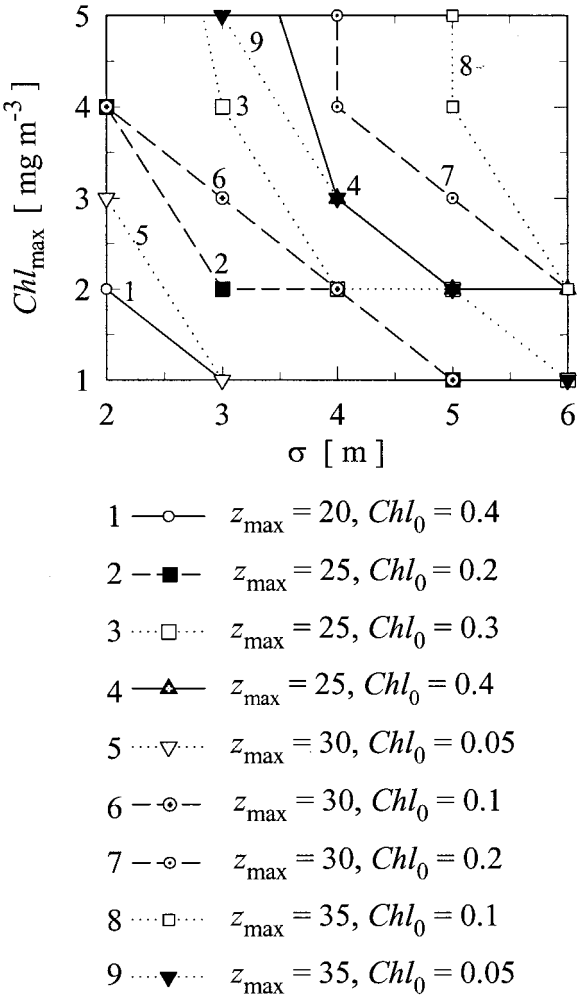

Fig. 6. Same as Fig. 4 but for $R_{rs}(485)/R_{rs}(555)$.

significantly affect the relationship between surface Chl and the reflectance ratio. In this figure several data points acquired under conditions when the relationship was significantly affected by the nonuniform Chl(z) profile are highlighted. It can be clearly seen that these data points depart considerably from the main body of data. For a given surface Chl, the measured $R_{rs}(442)/R_{rs}(555)$ is reduced because of the influence of the subsurface Chl maximum, which is consistent with our modeling results. As discussed above, the subsurface Chl maxima at stations z1 and z3 are not expected to affect the reflectance significantly. This conclusion is supported by Fig. 8, as the z1 and z3 data points are consistent with the main body of data. Figure 8 also shows that the OC4 (version 4) algorithm[10] does not provide the best fit to the data set presented in this figure.

5. Conclusions

The empirical ocean color algorithms for estimating Chl are typically based on the correlation between the measured spectral reflectances, R_{rs}, and the measured surface Chl. This type of correlation does not account for the vertical structure of inherent optical properties. Two bodies of water with the same surface Chl but different vertical distributions of Chl(z) and associated IOPs may have different values of $R_{rs}(\lambda)$ at any wavelength λ or different spectral ratios of R_{rs}. Therefore the vertical distribution of Chl(z) may introduce errors into the algorithm-derived surface chlorophyll. By using an approach based on radiative transfer simulations we showed that the percent difference in $R_{rs}(\lambda)$ or in the spectral ratios of $R_{rs}(\lambda)$ between a vertically inhomogeneous ocean (with the surface Chl identical to the homogeneous case) and a homogenous ocean can be significantly larger than 5% in many situations (Figs. 3–6). The magnitude of these differences depends strongly on the parameters that describe the Chl(z) profile. The absolute value of the difference exceeded 70% for a low surface Chl of 0.02 mg m^{-3} and a shallow depth of 20 m of the Chl maximum. When the surface Chl was greater than 0.4 mg m^{-3} or when the depth of the Chl maximum, z_{max}, was greater than 45 m (or 65 m in extremely clear waters with the surface Chl $\leq$ 0.02 mg m^{-3}), the effect on the blue-to-green reflectance ratio was less than 5% relative to the homogeneous ocean.

It is difficult to assess to what extent the nonuniform Chl(z) profile might affect the performance of the present empirical algorithms such as OC4, OC2 (Ocean chlorophyll 2),[10] or chlor_MODIS used in conjunction with global processing of SeaWiFS and MO-

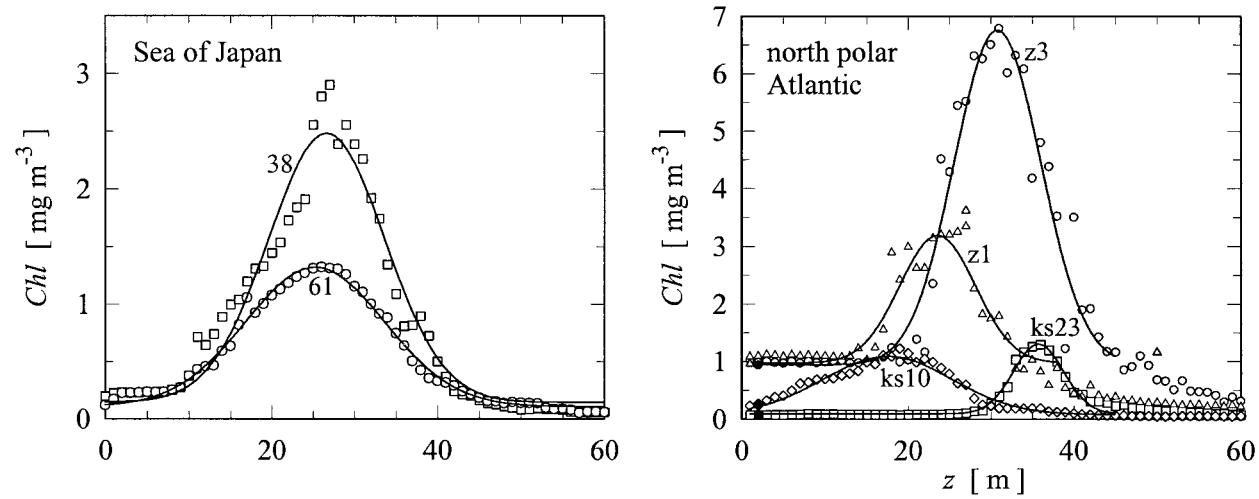

Fig. 7. Examples of the measured Chl(z) profiles from the Sea of Japan and the north polar waters of the Atlantic Ocean. Data points are accompanied by solid curves that represent the fitted Gaussian curves [Eq. (6)]. The dates, times, and locations of measurements and the parameters of the Gaussian curves are listed here. Station 38: 30 June 1999; 23:05 GMT; 38°01′N 128°53′E. h = 41.30, σ = 7.05, z_{max} = 26.5, Chl_0 = 0.15. Station 61: 5 July 1999; 2:16 GMT; 40°10′N 136°20′E. h = 25.62, σ = 8.45, z_{max} = 25.0, Chl_0 = 0.10. Station ks10: 15 July 1998; 6:49 GMT; 78°55′N 7°09′E. h = 19.80, σ = 7.80, z_{max} = 17.5, Chl_0 = 0.08. Station ks23: 16 July 1998; 15:35 GMT; 78°50′N 9°30′E. h = 9.25, σ = 3.0, z_{max} = 35.7, Chl_0 = 0.09. Station z1: 25 July 1999; 15:45 GMT; 78°00′N 5°00′E. h = 25.51, σ = 4.60, z_{max} = 20.3, Chl_0 = 0.97. Station z3: 25 July 1999; 7:30 GMT; 78°04′N 7°00′E. h = 76.16, σ = 5.22, z_{max} = 30.8, Chl_0 = 0.94.

DIS imagery. These algorithms are based on a large amount of field data that were collected in various oceanic regions throughout different seasons. It is likely that some of these data were collected in the presence of significant effects of a nonuniform Chl(z) profile on ocean reflectance, and some data were collected in the absence of such effects or under nearly homogeneous conditions in the upper ocean layer. Let us consider two extreme situations when the nonuniform Chl(z) profile may introduce errors into the algorithm-derived surface Chl. First, if field data with a substantial influence of the chlorophyll maximum on the measured R_{rs} values were included in the algorithm development to the extent that they significantly affected the algorithm, then the resultant formula for the algorithm would tend to provide lower values of the blue-to-green R_{rs} ratio than what would be observed in a homogeneous ocean with surface chlorophyll Chl_0. Therefore, if such an algorithm were applied to the satellite-derived reflectance for the pixels for which the Chl(z) profile is uniform or has no effect on ocean reflectance, the result would be an underestimation of surface Chl. The second hypothetical situation represents the case when the in-water algorithm is developed by use of field data that represent the uniform Chl(z) profiles or no effect of nonuniform profiles on ocean reflectance. If such an algorithm were applied to the satellite-derived reflectance for the pixels where the influence of the nonuniform Chl(z) profile was significant, the retrieved surface Chl would be overestimated.

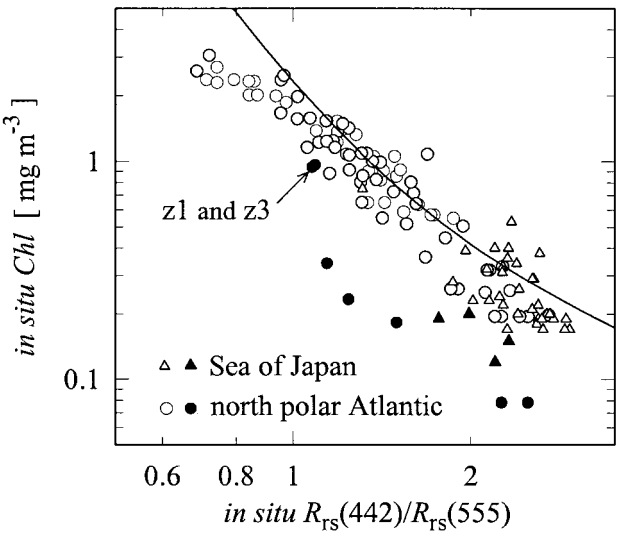

Fig. 8. Relationship between *in situ*-measured reflectance ratio $R_{rs}(442)/R_{rs}(555)$ and the measured chlorophyll a concentration at the sea surface. The data were collected in the Sea of Japan and the north polar Atlantic. Filled symbols indicate data collected when the remote-sensing reflectance was significantly affected by the nonuniform pigment profile (with the exception of the z1 and z3 stations; see text for an explanation). The solid curve shows the OC4 (version 4) algorithm.[10]

Figure 9 provides insight into the relationship between the OC4 and OC2 algorithms and the data affected by nonuniform Chl(z) profiles. This figure compares the OC4 and OC2 curves with the data from our radiative transfer simulations. For a given surface Chl, the rightmost data points correspond to our simulations with negligible effect of the nonuniform Chl(z) profile on the blue-to-green reflectance ratio. The solid curves that are close to these rightmost data points represent the reference simulations of a homogeneous ocean. The general slope of the solid curves is different from the slope of OC4 and OC2 lines. This indicates some systematic differences

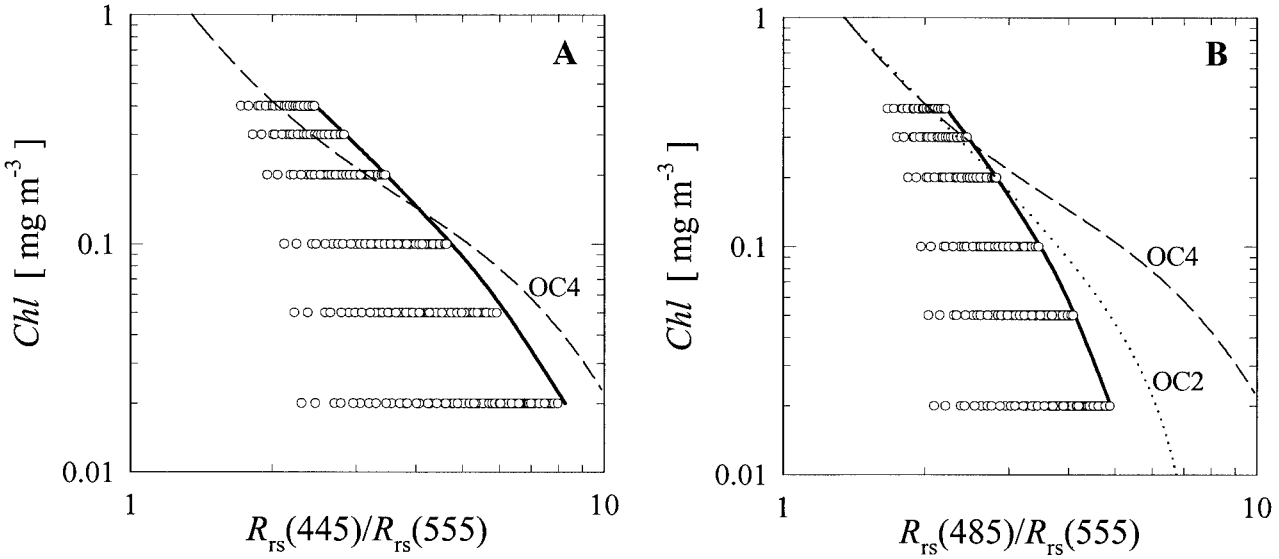

Fig. 9. A, Chlorophyll concentration at the sea surface, Chl, as a function of the blue-to-green ratio of remote-sensing reflectance $R_{rs}(445)/R_{rs}(555)$. B, Same as A but for $R_{rs}(485)/R_{rs}(555)$. The data points were obtained from our radiative transfer simulations for nonuniform pigment profiles, in which the absorption and scattering coefficients varied with depth (see text for a detailed explanation). Solid curves correspond to simulations of a homogeneous ocean. These curves are very close to the rightmost data points that represent simulations with negligible effect of nonuniform Chl(z) profiles on the reflectance ratio. The spread of the data points to the left from the solid curves illustrates the effects of nonuniform Chl(z) profiles in the simulations. For comparison, the OC4 (version 4) and OC2 (version 4) algorithms are shown.[10]

in the surface Chl-versus-reflectance ratio relationships between the databases that underlie the OC4 and OC2 algorithms and our simulations of homogeneous ocean. These differences may be due to the fact that the radiative transfer computations simulated a specific range of conditions (in terms of both in-water properties and boundary conditions) that was not so broad as that experienced in the collection of field data for the OC4 and OC2 algorithm development.

Regardless of these differences, an important result shown in Fig. 9 is that most data points from our modeling of the nonuniform Chl(z) profiles lie on the left-hand side of the OC4 and OC2 curves. This result is especially well pronounced for relatively low values of surface Chl (<0.2 mg m^{-3}). It indicates that the application of an OC4 or an OC2 algorithm when the nonuniform Chl(z) profile influences the reflectance ratio at low surface chlorophyll concentrations can lead to substantial overestimation in the algorithm-derived surface Chl. The extreme data point from our simulations that corresponds to the surface Chl = 0.02 mg m^{-3} and the blue-to-green (485 nm/555 nm) reflectance ratio of $\sim$2 suggests that this overestimation can be as high as 20-fold.

The internal inconsistency associated with correlating the surface value of Chl with reflectance values that depend on the vertical structure of inherent optical properties will continue to produce errors in the estimation of surface Chl from the current ocean-color algorithms. One possible but difficult and laborious approach to overcoming or at least minimizing this problem could be based on a development of regional algorithms with carefully chosen surface data for which detailed vertical profiles are known.[12] The application of such specific algorithms to satellite data in combination with knowledge of the typical vertical structure of the water column for a given region and season may then yield the best possible satellite-derived pigment concentration. It has been shown that, within regions and seasons, the vertical pigment profile in the open ocean can be a predictable property,[31] but more study will be needed for a better understanding of the variability in pigment profiles and eventually for incorporating such information into the development of remote-sensing algorithms.

This research was supported by NASA grants NAG5-12396 and NAG5-12397 (awarded to M. Stramska and D. Stramski) and U.S. Office of Naval Research grant N00014-98-1-0247 of the Japan–East Sea Departmental Research Initiative (awarded to B. G. Mitchell and D. Stramski). We thank B. G. Mitchell for making available the Sea of Japan data and the researchers from the Institute of Oceanology, Polish Academy of Sciences, as well as the officers and crews of R/V Oceania for assistance in the collection of data in the north polar Atlantic. We also thank W. S. Pegau and anonymous reviewers for useful comments on the manuscript.

References

1. H. R. Gordon and W. R. McCluney, "Estimation of the depth of sunlight penetration in the sea for remote sensing," Appl. Opt. **14,** 413–416 (1975).
2. R. C. Smith, "Remote sensing and depth distribution of ocean chlorophyll," Mar. Ecol. Prog. Ser. **5,** 359–361 (1981).
3. H. R. Gordon and O. B. Brown, "Diffuse reflectance of the

ocean: some effects of vertical structure," Appl. Opt. **14,** 2892–2895 (1975).
4. H. R. Gordon, "Remote sensing of optical properties in continuously stratified waters," Appl. Opt. **17,** 1893–1897 (1978).
5. H. R. Gordon and D. K. Clark, "Remote sensing optical properties of a stratified ocean: an improved interpretation," Appl. Opt. **19,** 3428–3430 (1980).
6. H. R. Gordon, "Diffuse reflectance of the ocean: influence of nonuniform phytoplankton pigment profile," Appl. Opt. **31,** 2116–2129 (1992).
7. A. Morel and L. Prieur, "Analysis of variations in ocean colour," Limnol. Oceanogr. **22,** 709–722 (1977).
8. H. R. Gordon and A. Morel, *Remote Assessment of Ocean Color for Interpretation of Satellite Visible Imagery—A Review*, lecture notes on coastal and estuarine studies (Springer-Verlag, Berlin, 1983).
9. J. E. O'Reilly, S. Maritorena, B. G. Mitchell, D. A. Siegel, K. L. Carder, S. A. Garver, M. Kahru, and C. McClain, "Ocean color chlorophyll algorithms for SeaWiFS," J. Geophys. Res. **103,** 24,937–24,953 (1998).
10. J. E. O'Reilly, S. Maritorena, D. Siegel, M. O'Brien, D. Toole, B. G. Mitchell, M. Kahru, F. P. Chavez, P. Strutton, G. Cota, S. Hooker, C. McClain, K. Carder, F. Muller-Karger, L. Harding, A. Magnuson, D. Phinney, G. Moore, J. Aiken, K. Arrigo, R. Letelier, and M. Culver, "Ocean color chlorophyll *a* algorithms for SeaWiFS, OC2, and OC4: version 4," in *SeaWiFS Postlaunch Calibrations and Validation Analyses, Part 3*, S. B. Hooker and E. R. Firestone, eds., NASA Tech. Memo. 2000-206892 (2000), Vol. 11, pp. 9–23.
11. D. K. Clark, National Oceanic and Atmospheric Administration, National Environmental Satellite Service, Washington, D.C. 20233 (personal communication, 2003).
12. S. Sathyendranath and T. Platt, "Remote sensing of ocean chlorophyll: consequence of nonuniform pigment profile," Appl. Opt. **28,** 490–495 (1989).
13. J. R. V. Zaneveld, "Remotely sensed reflectance and its dependence on vertical structure: a theoretical derivation," Appl. Opt. **21,** 4146–4150 (1982).
14. V. I. Haltrin, "Diffuse reflection coefficient of a stratified sea," Appl. Opt. **38,** 932–936 (1999).
15. O. Frette, S. R. Erga, J. J. Stamnes, and K. Stamnes, "Optical remote sensing of waters with vertical structure," Appl. Opt. **40,** 1478–1486 (2001).
16. C. D. Mobley, *Light and Water, Radiative Transfer in Natural Waters* (Academic, San Diego, Calif., 1994).
17. C. D. Mobley, *Hydrolight 4.1 User's Guide* (Sequoia Scientific, Mercer Island, Wash., 1999).
18. R. M. Pope and E. S. Fry, "Absorption spectrum (380–700 nm) of pure water. II. Integrating cavity measurements," Appl. Opt. **36,** 8710–8723 (1997).
19. F. M. Sogandares and E. S. Fry, "Absorption spectrum (340–640 nm) of pure water. I. Photothermal measurements," Appl. Opt. **36,** 8699–8709 (1997).
20. L. Prieur and S. Sathyendranath, "An optical classification of coastal and oceanic waters based on the specific spectral absorption curves of phytoplankton pigments, dissolved organic matter, and other particulate materials," Limnol. Oceanogr. **26,** 671–689 (1981).
21. A. Morel, "Light and marine photosynthesis: a spectral model with geochemical and climatological implications," Prog. Oceanogr. **26,** 263–306 (1991).
22. R. C. Smith and K. Baker, "Optical properties of the clearest natural waters," Appl. Opt. **20,** 177–184 (1981).
23. T. J. Petzold, "Volume scattering functions for selected ocean waters," Tech. Rep. (Scripps Institution of Oceanography, University of California, San Diego, La Jolla, Calif., 1972).
24. M. R. Lewis, J. J. Cullen, and T. Platt, "Phytoplankton and thermal structure of the upper ocean: consequences of nonuniformity in the chlorophyll profile," J. Geophys. Res. **88,** 2565–2570 (1983).
25. T. Platt, S. Sathyendranath, C. M. Caverhill, and M. R. Lewis, "Ocean primary production and available light: further algorithms for remote sensing," Deep-Sea Res. **35,** 855–879 (1988).
26. J. C. Kitchen and J. R. V. Zaneveld, "On the noncorrelation of the vertical structure of light scattering and chlorophyll *a* in case 1 waters," J. Geophys. Res. **95,** 20,237–20,246 (1990).
27. W. E. Esaias, M. R. Abbott, I. Barton, O. B. Brown, J. W. Campbell, K. L. Carder, D. K. Clark, R. H. Evans, F. E. Hoge, H. R. Gordon, W. M. Balch, R. Letelier, and P. J. Minnett, "An overview of MODIS capabilities for ocean Science observations," IEEE Trans. Geophys. Remote Sens. **36,** 1250–1265 (1998).
28. J. L. Mueller and R. W. Austin, "Ocean optics protocols for SeaWiFS validation, revision 1," NASA Tech. Memo. 104566 (1995).
29. M. Stramska, D. Stramski, R. Hapter, S. Kaczmarek, and J. Ston, "Bio-optical relationships and ocean color algorithms for the north polar region of the Atlantic," J. Geophys. Res. **108**(C5), 3143, doi: 10.1029/2001JC001195 (2003).
30. C. C. Trees, R. R. Bidigare, D. M. Karl, and L. Van Heukelem, "Fluorometric chlorophyll *a*: Sampling, laboratory methods, and data analysis protocols," in *Ocean Optics Protocols for Satellite Ocean Color Sensor Validation, Revision 2*, G. S. Fargion and J. L. Mueller, eds., NASA Tech. Memo. 2000-209966 (2000), pp. 162–169.
31. T. Platt and S. Sathyendranath, "Oceanic primary production: estimation by remote sensing at regional and larger scales," Science **241,** 1613–1620 (1988).